Journal of Colloid and Interface Science 398 (2013) 234–239

Contents lists available at SciVerse ScienceDirect

Journal of Colloid and Interface Science

www.elsevier.com/locate/jcis

Enhanced photocatalytic degradation of methylene blue on multiwalled carbon nanotubes–TiO_2

Donglin Zhao [a,b,*], Xin Yang [b], Changlun Chen [b,*], Xiangke Wang [b]

[a] School of Materials and Chemical Engineering, Anhui University of Architecture, Hefei, Anhui 230601, PR China
[b] Key Laboratory of Novel Thin Film Solar Cells, Institute of Plasma Physics, Chinese Academy of Sciences, P.O. Box 1126, Hefei 230031, PR China

ARTICLE INFO

Article history:
Received 24 December 2012
Accepted 8 February 2013
Available online 22 February 2013

Keywords:
MWCNT/TiO_2
Visible-light photocatalyst
Degradation

ABSTRACT

A visible-light photocatalyst of multiwalled carbon nanotubes decorated with TiO_2 nanoparticles (MWCNT/TiO_2) was synthesized by a two-step method, in which TiO_2 was first mounted on MWCNT surfaces by hydrolysis of tetrabutyl titanate and further crystallized into anatase nanocrystal in a vacuum furnace at 500 °C. The photocatalytic degradation of methylene blue over the ultraviolet (UV) and visible-light spectrum regions was investigated. The MWCNT/TiO_2 was able to absorb a high amount of photo energy in the visible-light region, driving effectively photochemical degradation reactions. There were more ·OH radicals produced by the MWCNT/TiO_2 (1:3) than by pure TiO_2 under UV and visible-light irradiation. In the photodegradation of methylene blue, as a model reaction, a signification enhancement in the reaction rate was observed with the MWCNT/TiO_2 (1:3), compared to bare TiO_2 and the physical mixture of MWCNTs and TiO_2. MWCNTs can improve the photocatalytic activity of TiO_2 in two aspects, namely e^- transportation and adsorption. This work provides new insight into the fabrication of MWCNT/TiO_2 as a high performance visible-light photocatalyst and facilitates its application in photocatalytic degradation of organic compounds.

1. Introduction

The photocatalytic degradation of organic compounds has attracted much attention due to its potential to purify wastewater that is discharged from industry and households [1]. Heterogeneous photocatalysts offer great potential for converting photon energy into chemical energy and therefore decomposing organic contaminants. A typical example is the TiO_2-based photocatalytic detoxification of air and water for environmental remediation [2,3]. However, there are still many challenges that are yet to be met before these photocatalysts become economically feasible. Difficulties include the enhancement of solar energy conversion and the suppression of the recombination of photogenerated electron–hole pairs.

In recent years, much effort has been exerted on constructing visible-light driven TiO_2 because of its obvious merit on the solar energy utilization. Modifying TiO_2 with a carbonaceous substance on the surface can induce visible-light responsive activity [4–6]. Various types of carbon, such as graphitic or coke-like carbon [5,6] or carbonate structural fragments bonding with TiO_2 [7], are proposed as the origin of the visible-light activity. Carbon materials have some beneficial effects on the photocatalytic activity of TiO_2 by inducing synergies or cooperative effects between the metal oxide and the carbon phases [8–11]. Much effort to combine TiO_2 with carbon nanotubes (CNTs) [12] in mixtures or as composite materials sought to create more highly reactive photocatalysts [10,13–15]. The synthesis of TiO_2/CNT composites using sol–gel, chemical vapor deposition, and physical vapor deposition methods has been reported [14,16–19]. The addition of multiwalled CNTs (MWCNTs) to a slurry of Degussa P25 improved color removal in aqueous solution of azo-dyes under ultraviolet (UV) light irradiation [16]. The researchers, however, did not fully explain how CNT/TiO_2 interacted to accelerate the decay of the dye. MWCNTs coated with a uniform layer of anatase TiO_2 displayed a higher rate of phenol degradation than either of the components alone or in simple mixtures [10]. The researchers proposed that the MWCNTs served as a catalyst-support increasing the reactive surface area of the TiO_2, and that intimate interphase contact between the TiO_2 and the MWCNTs has other synergistic photochemical effects. The researchers indicated that MWCNTs not only provided a large surface area support for the titania catalyst, but also stabilized the charge separation by trapping the electrons transferred from TiO_2, thereby hindering charge recombination. Given the conducting and semiconducting properties of CNTs, it is also possible that photoexcited electrons from TiO_2 may be transferred to the CNTs to hinder recombination and enhance oxidative reactivity. There are some

* Corresponding authors. Address: School of Materials and Chemical Engineering, Anhui University of Architecture, Hefei, Anhui 230601, PR China (D. Zhao). Fax: +86 551 65591310.
E-mail addresses: zhaodlin@126.com (D. Zhao), clchen@ipp.ac.cn (C. Chen).

0021-9797/$ - see front matter © 2013 Elsevier Inc. All rights reserved.
http://dx.doi.org/10.1016/j.jcis.2013.02.017

reports on the photocatalytic degradation of methylene blue (MB) on carbon-modified TiO_2 photocatalysts [20–23]. The mechanisms for the enhanced reactivity of CNT/TiO_2, especially under visible-light irradiation, were not fully investigated by the spectroscopic characterization such as the ultraviolet–visible (UV–Vis) spectrum, X-ray photoelectron spectroscopy (XPS), the photoluminescence (PL) excitation and emission spectrum, the electron paramagnetic resonance (EPR), and spin trap techniques. Therefore, the mechanisms for the enhanced reactivity of CNT/TiO_2 are necessary to be further studied. The effect of the mass ratio of CNTs on TiO_2 on the efficiency of MB degradation is very important and also necessary to be further studied.

In this work, the MWCNT/TiO_2 visible-light responsive photo catalyst was prepared by a two-step method, in which TiO_2 was first mounted on MWCNT surfaces by hydrolysis of tetrabutyl titanate and further crystallized into anatase nanocrystal in a vacuum furnace at 600 °C. The photocatalytic degradation of methylene blue (MB), as a representative of organic compounds because of its ubiquitous present in factory wastewater, was investigated over the UV and visible-light spectrum regions. The MWCNT/TiO_2 is able to absorb a high amount of photo energy in the visible-light region, driving effectively photochemical degradation reactions. The mechanisms for the enhanced photocatalytic reactivity of MWCNT/TiO_2 were explored with UV–Vis spectrum, XPS spectrum, the PL excitation and emission spectrum, and the EPR spin trap techniques.

2. Experimental

All reagents were analytical grade and were used as received. Milli-Q (Millipore, Billerica, MA, USA) water was used in all experiment. MWCNTs were prepared by chemical vapor deposition of acetylene in a hydrogen flow at 760 °C using Ni–Fe nanoparticles as catalysts, followed by oxidation with 1 M HNO_3.

2.1. Preparation of MWCNT/TiO_2

One gram oxidized MWCNTs were dispersed in a solution of Milli-Q water (100 mL) and ethanol (100 mL) by ultrasonic treatment for 10 min, and then, a mixture solution (100 mL) of $Ti(OC_4H_9)_4$ and ethanol were slowly added into the above suspension and stirred for 1 h. After that, the solvent (mixture of ethanol and water) was evaporated out at 90 °C. Thus prepared TiO_2-mounted MWCNTs were calcinated in a vacuum furnace at 600 °C for 1 h. For comparison, we simultaneously prepared pure TiO_2 without MWCNTs.

2.2. Characterization

Morphology and particle size of the MWCNT/TiO_2 were visualized using a JSM-6700F scanning electron microscope (SEM) and a JEM-2010 transmission electron microscope (TEM). XRD patterns were recorded in reflection mode (Cu Kα radiation, λ = 1.5418 Å) on a Scintag XDS-2000 diffractometer. UV–Vis spectra were recorded on a Shimadzu UV-2550 spectrophotometer equipped with a Labsphere diffuse reflectance accessory. XPS spectra were obtained with an ESCALab220i-XL electron spectrometer from VG Scientific using 300 W Al Kα radiation. The photoluminescence, PL, and excitation and emission spectra were taken on a FL/FS 900 time-resolved fluorescence spectrometer. Electron spin resonance (ESR) spectra were obtained using a Bruker model ESP 300E ESR spectrometer. The settings for the ESR spectrometer were center field 3480.00 G, microwave frequency 9.79 GHz, and power 5.05 mW.

2.3. Photocatalytic experiment

A 125 W mercury lamp was positioned inside a cylindrical vessel, surrounded by a circulating water jacket for cooling. 50 mg of photocatalyst was suspended in 100 mL aqueous solution of 10 mg L^{-1} MB. The solution was stirred in dark for 2 h to ensure the establishment of an adsorption–desorption equilibrium. The probe was then irradiated with visible-light using cutoff filter (λ > 450 nm). During the irradiation, 2 mL aliquots were removed at certain time intervals and analyzed with a Shimadzu UV-2550 spectrophotometer to record MB concentrations.

3. Results and discussion

3.1. Characterization of MWCNT/TiO_2

Fig. 1 shows the morphology and inner structure of MWCNT/TiO_2. SEM and TEM images (Fig. 1A and B) show a sample with nanotubes covered homogeneously with TiO_2, having a diameter ranging from 10 to 15 nm, and no TiO_2 aggregates are observed. In the case of MWCNTs/TiO_2, due to preferential heterogeneous nucleation, a very uniform shell consisting of tiny TiO_2 nanoparticles (Fig. 1A and B), deposits on the MWCNTs, whose surface contains an abundance of hydroxyl groups, carboxyl groups, and carbonyl groups [19].

XRD patterns (Fig. 1C) show that MWCNT/TiO_2 seems to be quite well crystallized. For the physical mixture of MWCNTs and TiO_2 (1:3), there is obvious peak at 2θ = 26.2°, corresponding to MWCNTs. The structure of MWCNTs and TiO_2 is different from the structure of the physical mixture of MWCNTs and TiO_2. This demonstrates that indeed, MWCNTs play a supporting role in the formation of the crystalline phase through crystallite surface stabilization.

The information regarding the chemical and bonding environment of MWCNT/TiO_2 was ascertained using XPS (Fig. 1D–F). With respect to the XPS O 1s spectra in Fig. 1E, four peaks at 530.4, 531.3, 532.17, and 533.77 eV have been fitted, which are ascribed to Ti—O—Ti (lattice O), C=O (and COO), Ti—OH, and C—OH (and C—O—C) species, respectively [24,25]. The main C 1s peak in Fig. 1F is dominated by elemental carbon at 284.6 eV, attributed mainly to sp^2 hybridized carbon (BE = 284.6 eV). The weak C 1s peak at 285.2 eV is attributed mainly to sp^3 hybridized carbon, and two weak peaks at 286.3 and 288.9 eV are assigned to the oxygen bound species C—O and O—C=O, respectively [26,27]. No C 1s peak at ~281 eV (Ti—C bond) [28] is observed, and the chemical environments for Ti and O are not changed, strongly suggesting that carbon atom does not directly enter into bulk TiO_2 lattice. This is not expected as many conventional C-doped TiO_2 is synthesized at temperatures higher than 600 °C [28–30]. Under crystallization conditions used herein, it is thought that TiO_2 is grafted onto the MWCNT surfaces via C—O—Ti bond, with such structure favoring the desired charge transfer upon light excitation [31]. C—O—Ti bond extends the light absorption to longer wavelengths.

UV–Vis diffuse reflectance spectroscopy confirms that the MWCNT/TiO_2 can adsorb significantly more light in the 420–800 nm region as compared with pure TiO_2, and the physical mixture of MWCNTs and TiO_2 (1:3) (Fig. 2A). The TiO_2 band gap is obviously smeared out to longer wavelengths, whilst the composite spectrum has changed, more in the visible range observed concurrently with less extinction in the infrared region. The enhancement of absorption in the visible range increases with increasing MWCNT ratio in the MWCNT/TiO_2. The combination of MWCNTs and TiO_2 gives rise to synergistic properties arising from the beneficial interaction of the two.

The PL emission spectrum has been widely used to investigate the efficiency of charge carrier trapping, immigration and transfer,

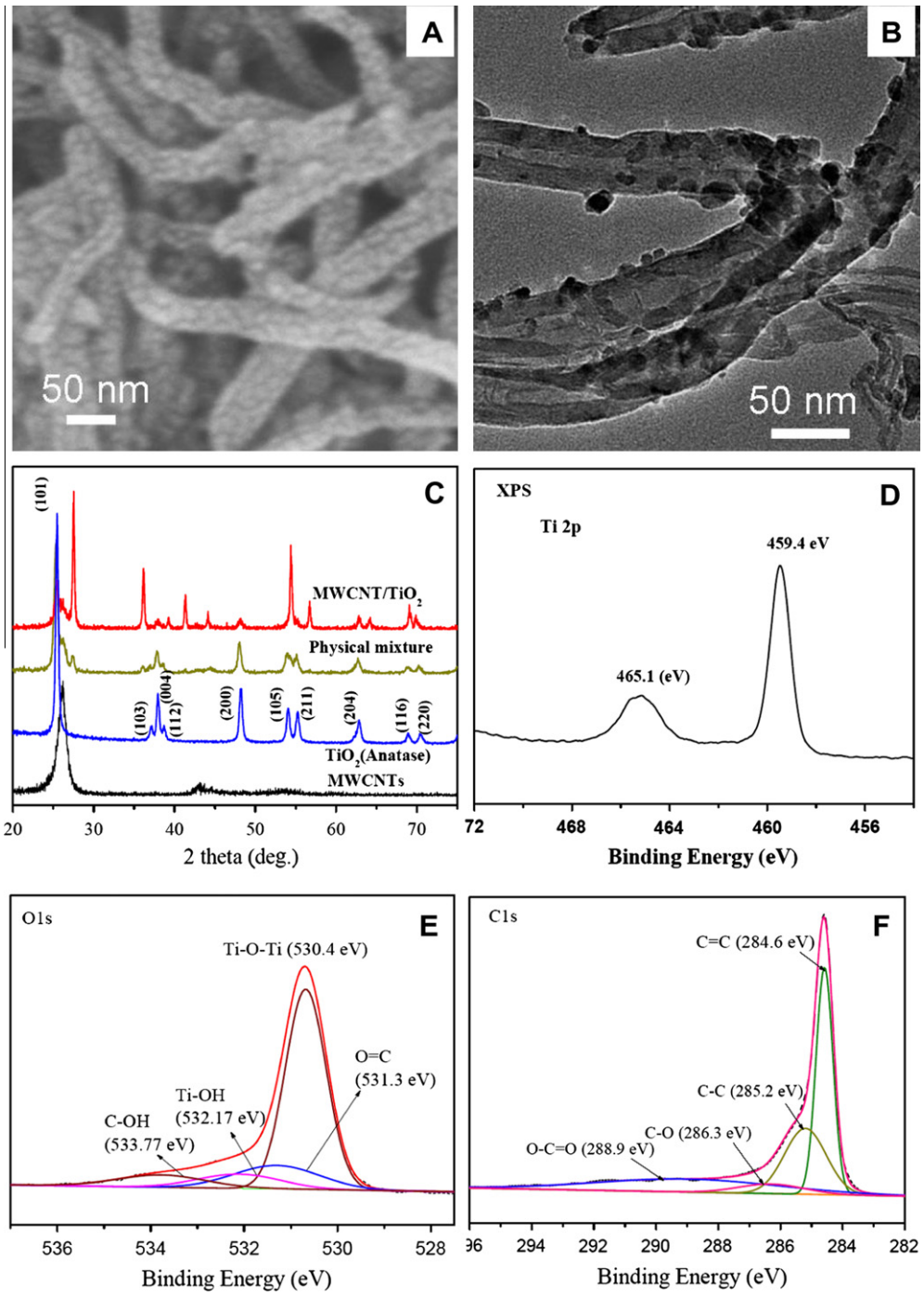

Fig. 1. SEM (A), TEM (B), XRD patterns (C), and high resolution Ti (D) O (E), and C (F) XPS of the MWCNT/TiO_2.

and to understand the fate of e^-/h^+ pairs in semiconductor particles [32]. With the recombination of e^-/h^+ after a photocatalyst is irradiated, photons are emitted, resulting in the photoluminescence. This behavior is attributed to the reverse radiative deactivation from the excited-state of Ti species. In order to study the effect of MWCNTs on the recombination of e^-/h^+ produced by TiO_2, the PL shown in Fig. 2B compares the e^-/h^+ recombination of MWCNT/TiO_2 to TiO_2, MWCNTs, and the physical mixture of MWCNTs and TiO_2. TiO_2 powder shows a broad PL emission band, which is similar to the results in the earlier study [33]. The emission band corresponding to the peak position of ~520 nm is for anatase powder [34]. As expected, no PL signal is observed in the range of 500–600 nm for MWCNTs. MWCNT/TiO_2 shows diminished PL intensity indicating reduced charge recombination in comparison with TiO_2 alone. This reduction increases with increasing MWCNTs ratio in the MWCNT/TiO_2. Peak shifts are caused by the trapping of electrons at defect sites prior to recombination [34]. For the physical mixture of MWCNTs and TiO_2, there is only slight PL intensity reduction, indicating the structure of MWCNT/TiO_2 is important for recombination reduction.

3.2. Photodegradation of MB

The photocatalytic activities of MWCNTs, pure TiO_2, the physical mixture of MWCNTs and TiO_2, and the MWCNT/TiO_2 were measured by the photodegradation of MB under UV and visible-light

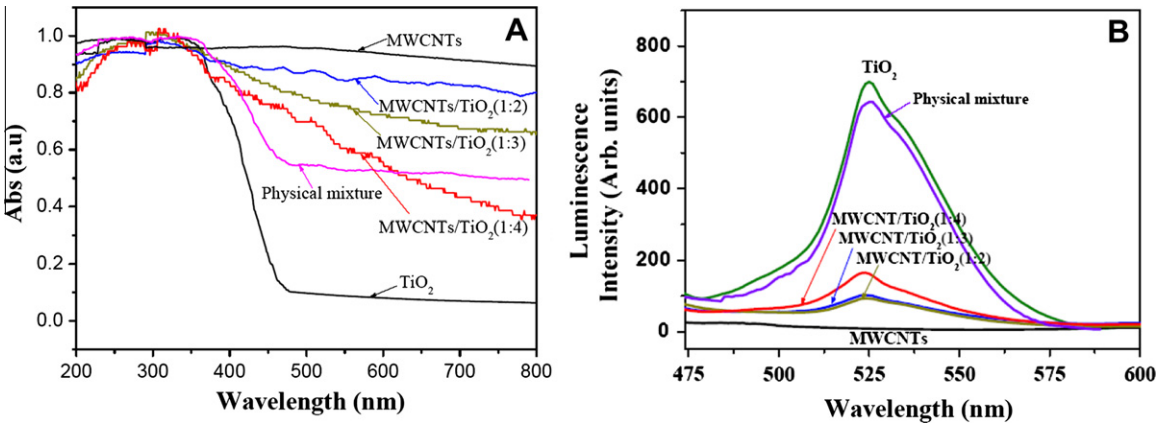

Fig. 2. (A) UV–Vis diffuse reflectance spectra, and (B) PL spectra of MWCNTs, TiO_2, physical mixture of MWCNTs and TiO_2 (1:3), and MWCNT/TiO_2.

($\lambda > 450$ nm), and the results are shown in Fig. 3A and B, respectively. The normalized temporal concentration changes (C/C_o) of MB during the photodegradation are proportional to the normalized maximum absorbance (A/A_o) and derived from the changes in MB's absorption profile ($\lambda = 633$ nm) at a given time interval. It is clear from Fig. 3A that the MWCNT/TiO_2 shows significant progress in the photodegradation of MB compared to MWCNTs, pure TiO_2, the physical mixture of MWCNTs and TiO_2 (1:3), and it also exhibits the highest efficiency at the mass ratio of MWCNTs:TiO_2 = 1:3. These results are consistent with previous studies that a suitable loading content of MWCNTs is crucial for optimizing the photocatalytic activity of MWCNTs/TiO_2 [19].

Under UV light irradiation, about 76% MB is decomposed by the MWCNT/TiO_2 (1:3) after less than 100 min. Contrastingly, 30–40% MB still remains in the solution after the same time period for pure TiO_2, the physical mixture of MWCNTs and TiO_2 (1:3). In addition, in the visible-light photodegradation (Fig. 3B), pure TiO_2 shows rather poor photocatalytic activity due to its limited photoresponding range and only 13% of the initial MB diminishes after more than 100 min. The photodegradation rate of the physical mixture of MWCNTs and TiO_2 is 17% after irradiation time of 100 min at $\lambda > 450$ nm. Whereas the MWCNT/TiO_2 (1:3) shows remarkable improvement in the photodegradation rate, 52% of MB is decomposed. The MWCNT/TiO_2 shows the highest photocatalytic activity of all compared materials under light with a wavelength larger than 450 nm, respectively, thus proving that indeed a special performance is to be expected, because of the dyadic bonding between MWCNTs and TiO_2.

3.3. Mechanisms of the enhanced photocatalysis

EPR spin trap technique, using 5,5-dimethyl-1-pyrroline-*N*-oxide (DMPO) as the spin-trapping reagent, is well-known to be an efficient measurement method to determine ·OH. Fig. 4 shows the EPR spectra of DMPO-·OH spin adducts produced in the dispersion systems of MWCNTs, TiO_2, and MWCNT/TiO_2 (1:3) as easily identified by the classical 1:2:2:1 spectral signature of spin-trapped ·OH. Under UV irradiation, the intensity of the 1:2:2:1 spectral signature of the DMPO-·OH spin adducts for MWCNT/TiO_2 (1:3) is obviously stronger than that with TiO_2, and there is no 1:2:2:1 spectral signature of the DMPO-·OH spin adducts for MWCNTs. Under visible-light irradiation, there is no obvious 1:2:2:1 spectral signature of the DMPO-·OH spin adducts for TiO_2, whereas there is strong 1:2:2:1 spectral signature of the DMPO-·OH spin adducts for MWCNT/TiO_2 (1:3). Therefore, MWCNT/TiO_2 (1:3) is photocatalytically more active than TiO_2 because there are more ·OH radicals produced by MWCNT/TiO_2 (1:3) under UV and visible-light irradiation. It could be inferred that MB were eliminated mainly by means of ·OH radical oxidation under UV and visible-light irradiation.

The schematic mechanism illustration of the enhancement of photocatalytic activity for TiO_2 by MWCNTs is summarized in Fig. 5. From all experimental results mentioned above, it can be proposed that MWCNTs can enhance the photocatalytic activity of TiO_2 in two aspects, namely e^- transportation and adsorption. It is confirmed that the MWCNT/TiO_2 can induce the formation of hydroxyl radical under visible-light irradiation ($\lambda > 450$ nm). How-

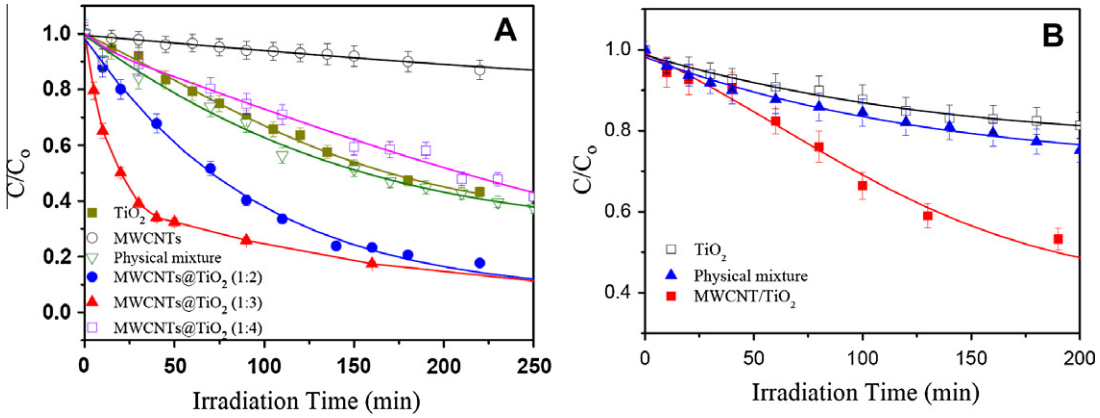

Fig. 3. Photocatalytic degradation of MB by MWCNTs, TiO_2, physical mixture of MWCNTs and TiO_2 (1:3), and MWCNT/TiO_2 under UV light (A). Photocatalytic degradation of MB by pure TiO_2, physical mixture of MWCNTs and TiO_2 (1:3), and MWCNT/TiO_2 (1:3) under visible-light (filter: $\lambda > 450$) (B).

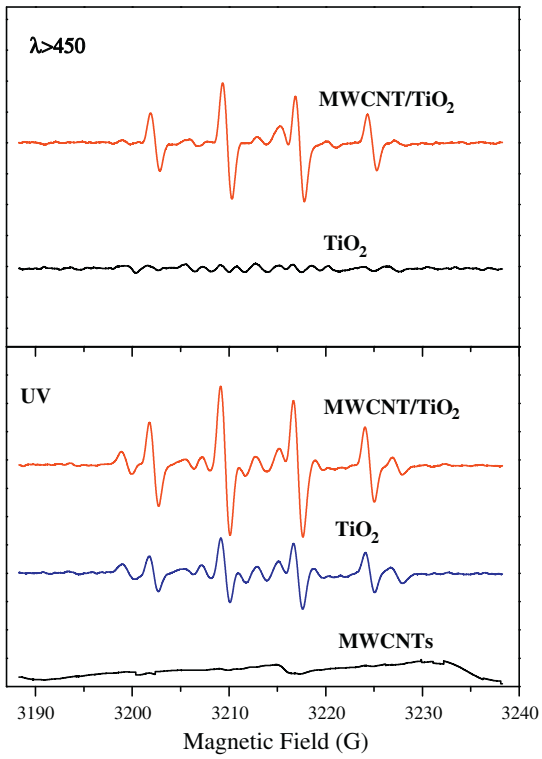

Fig. 4. The hydroxyl radical EPR spectra of MWCNTs, pure TiO_2, and MWCNT/TiO_2 (1:3) formed in aqueous dispersions in a Pyrex vessel after 2 min irradiation by UV and after 5 min irradiation by visible-light (filter: $\lambda > 450$). In the system, the catalyst loading is 0.5 g L^{-1}, and the concentration of DMPO is 0.4 mol L^{-1}.

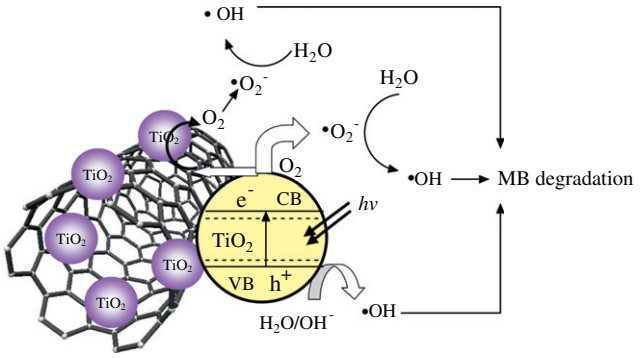

Fig. 5. The illustration of mechanisms of the activation of photocatalytic activity for MB by the MWCNT/TiO_2.

ever, this ability relies on the fact that the hole of the joint system is position near the TiO_2 valence band, as it needs ~2.4 V versus normal hydrogen electrode to drive the hydroxyl radical formation. This would be not possible for the usual sensitizing situation, which would fill the much less noble and therefore less reactive MWCNT sub-gaps. On the base of our experimental data, it is proposed that the synergistic dyade structure of MWCNT/TiO_2 provides access to optically active charge transfer transition. Under UV light irradiation, electrons (e^-) are excited from the valence band (VB) to the conduction band (CB) of TiO_2, creating a change vacancy, or hole (h^+), in the VB. In the absence of MWCNTs, most of these charges quickly recombine without doing any chemistry. Typically, only a small number of electrons (<1%) and holes are trapped and participate in photocatalytic reactions, resulting in low reactivity [35]. It has been reported that the CB position of anatase is about −4.21 eV using vacuum level as a reference, with a band gap of about 3.2 eV [36]. The work function of MWCNTs is similar to that of graphite, ~4.7 eV [37], depending sensitively on the number of layers. When TiO_2 nanoparticles are in intimate contact with MWCNTs, the relative position of the MWCNT CB edge permits the transfer of electrons from TiO_2 surface, allowing charge separation, stabilization, and recombination. The excited electrons can be shuttled freely along the conducting network of MWCNTs and subsequently transfer to the surface to react with water and oxygen to yield hydroxyl radical, which would oxidize MB. The longer-lived holes on TiO_2, then, account for the higher activity of the MWCNT/TiO_2 photocatalyst. Furthermore, the adsorption ability of TiO_2 bound to MWCNTs greatly increases due to more active sites available on the surfaces of MWCNTs. Since O_2 may be adsorbed on the surfaces of MWCNTs, the e^- in the MWCNTs reacts with O_2 and finally forms ·OH, which oxidizes the adsorbed MB directly on the surfaces. The routes of ·OH formation and the photodegradation of MB can be described as follows:

$$TiO_2 + h\nu \rightarrow (e^-_{CB}) + (h^+_{VB}) \rightarrow MWCNTs(e^-) + h^+ \quad (1)$$

$$TiO_2(h^+_{VB}) + OH^-_{ads} \rightarrow \cdot OH + TiO_2 \quad (2)$$

$$TiO_2(e^-_{CB}) + O_{2ads} \rightarrow \cdot O_2^- + TiO_2 \xrightarrow{H_2O} \cdot OH + TiO_2 \quad (3)$$

$$MWCNTs + (e^-) + O_{2ads} \rightarrow \cdot O_2^- + MWCNTs \xrightarrow{H_2O} \cdot OH + MWCNTs \quad (4)$$

$$MB_{ads} + \cdot OH \rightarrow \text{Degraded products} \quad (5)$$

The amount of ·OH formed in the system with TiO_2 bound to MWCNTs is more than that with TiO_2 alone as a photocatalyst. Moreover, MB molecules can transfer from solution to the catalyst's surfaces and be adsorbed with offset face-to-face orientation by π–π conjugation between MB and aromatic regions of the MWCNTs, and therefore, the adsorptivity of MB on MWCNTs increases compared to that of MB on bare TiO_2. Therefore, the MWCNT/TiO_2 has higher efficiency in photodegradation of MB compared to TiO_2 alone as a photocatalyst.

4. Conclusion

The results of this research highlighted the photocatalytic activities under UV and visible-light irradiation, mechanisms for the improved photocatalytic reactivity of the MWCNT/TiO_2. The MWCNT/TiO_2 has anatase phase and is able to absorb a high amount of photoenergy in the visible-light region, driving effectively photochemical degradation reactions. Photochemical characterization of the MWCNT/TiO_2 confirmed that the origin of photocatalytic activity under visible-light is due to a direct optical charge transition involving both TiO_2 and MWCNTs, keeping the high reactivity of the photogenerated electron and hole. The results of this research highlighted new insight into the fabrication of the MWCNT/TiO_2 as a high performance visible-light responsive catalyst and facilitates its application in environmental protection issues. Our findings are relevant and important for the use of the MWCNT/TiO_2 in photocatalytic degradation of organic compounds in environmental pollution cleanup.

Acknowledgments

Financial supports from the 973 project of MOST (2011CB933700), and the National Natural Science Foundation of China (21071147; 91126020; 21077107; 20971126) are acknowledged.

References

[1] M. Kaneko, I. Okura, in: M. Kaneko, I. Okura (Eds.), Photocatalysis, Kohdansha-Springer, Tokyo, Japan, 2002.
[2] J.C. Crittenden, Y. Zhang, D.W. Hand, D.L. Perram, E.G. Marchand, Water Environ. Res. 68 (1996) 270.
[3] N.V. Muradov, Sol. Energy 52 (1994) 283.
[4] C. Chen, M.C. Long, H. Zeng, W.M. Cai, B.X. Zhou, J.Y. Zhang, Y.H. Wu, D.W. Ding, D.Y. Wu, J. Mol. Catal. A 314 (2009) 35.
[5] C. Lettmann, K. Hildenbrand, H. Kisch, W. Macyk, W.F. Maier, Appl. Catal. B 32 (2001) 215.
[6] L.W. Zhang, H.B. Fu, Y.F. Zhu, Adv. Funct. Mater. 18 (2008) 2180.
[7] P. Zabek, J. Eberl, H. Kisch, Photochem. Photobiol. Sci. 8 (2009) 264.
[8] C.G. da Silva, J.L. Faria, J. Photochem. Photobiol. A 155 (2003) 133.
[9] B. Tryba, A.W. Morawski, M. Inagaki, Appl. Catal. B 41 (2003) 427.
[10] W.D. Wang, P. Serp, P. Kalck, J.L. Faria, Appl. Catal. B 56 (2005) 305.
[11] W.D. Wang, C.G. Silva, J.L. Faria, Appl. Catal. B 70 (2007) 470.
[12] S. Iijima, Nature 354 (1991) 56.
[13] Y. Yu, J.C. Yu, C.Y. Chan, Y.K. Che, J.C. Zhao, L. Ding, W.K. Ge, P.K. Wong, Appl. Catal. B 61 (2005) 1.
[14] W. Feng, Y.Y. Feng, Z.G. Wu, A. Fujii, M. Ozaki, K. Yoshino, J. Phys. Condens. Matter. 17 (2005) 4361.
[15] S.Z. Kang, Z.Y. Cui, J. Mu, Nanotubes, Carbon Nanostruct. 15 (2007) 81.
[16] W.G. Fan, L. Gao, J. Sun, J. Am. Ceram. Soc. 89 (2006) 731.
[17] A. Jitianu, T. Cacciaguerra, R. Benoit, S. Delpeux, F. Beguin, S. Bonnamy, Carbon 42 (2004) 1147.
[18] Y. Yao, G. Li, S. Ciston, R.M. Lueptow, K.A. Gray, Environ. Sci. Technol. 42 (2008) 4952.
[19] J.G. Yu, T.T. Ma, S.W. Liu, Phys. Chem. Chem. Phys. 13 (2011) 3491.
[20] H.B. Huang, D.Y.C. Leung, P.C.W. Kwong, J. Xiong, L. Zhang, Catal. Today 201 (2013) 189.
[21] E. Kusiak-Nejman, M. Janus, B. Grzmil, A.W. Morawski, J. Photochem. Photobiol. A 226 (2011) 68.
[22] J. Kasanen, J. Salstela, M. Suvanto, T.T. Pakkanen, Appl. Surface Sci. 258 (2011) 1738.
[23] A. Baraka, Water Treat. 49 (2012) 172.
[24] G.M. An, W.H. Ma, Z.Y. Sun, Z.M. Liu, B.X. Han, S.D. Miao, Z.J. Miao, K.L. Ding, Carbon 45 (2007) 1795.
[25] N.P. Zschoerper, V. Katzenmaier, U. Vohrer, M. Haupt, C. Oehr, T. Hirth, Carbon 47 (2009) 2174.
[26] E. Papirer, R. Lacroix, J.B. Donnet, G. Nansé, P. Fioux, Carbon 33 (1995) 63.
[27] W.J. Ren, Z.H. Ai, F.L. Jia, L.Z. Zhang, X.X. Fan, Z.G. Zou, Appl. Catal. B 69 (2007) 138.
[28] H. Irie, Y. Watanabe, K. Hashimoto, Chem. Lett. 32 (2003) 772.
[29] T. Tsumura, N. Kojitani, I. Izumi, N. Iwashita, M. Toyoda, M. Inagaki, J. Mater. Chem. 12 (2002) 1391.
[30] B. Tryba, A.W. Morawski, T. Tsumura, M. Toyoda, M. Inagaki, J. Photochem. Photobiol. A 167 (2004) 127.
[31] M. Niederberger, G. Garnweitner, F. Krumeich, R. Nesper, H. Colfen, M. Antonietti, Chem. Mater. 16 (2004) 1202.
[32] J.G. Yu, H.G. Yu, B. Cheng, X.J. Zhao, J.C. Yu, W.K. Ho, J. Phys. Chem. B 107 (2003) 13871.
[33] X.Z. Li, F.B. Li, C.L. Yang, W.K. Ge, J. Photochem. Photobiol. A 141 (2001) 209.
[34] K. Fujihara, S. Izumi, T. Ohno, M. Matsumura, J. Photochem. Photobiol. A: Chem. 132 (2000) 99.
[35] G.H. Li, K.A. Gray, Chem. Phys. 339 (2007) 173.
[36] Y. Xu, M.A.A. Schoonen, Am. Mineral. 85 (2000) 543.
[37] S.C. Lim, H.J. Jeong, K.S. Kim, I.B. Lee, D.J. Bae, Y.H. Lee, Carbon 43 (2005) 2801.